Detecting divertor damage during steady state operation of W7-X from thermographic measurements

A. Rodatos,[1, a)] H. Greuner,[2] M. W. Jakubowski,[1] J. Boscary,[2] G. A. Wurden,[3] T. S. Pedersen,[1] R. König,[1] and W7-X Team

[1)]*Max Planck Institute for Plasma Physics, Wendelsteinstr. 1, Greifswald, Germany*

[2)]*Max Planck Institute for Plasma Physics, Boltzmannstr. 2, Garching, Germany*

[3)]*Los Alamos National Laboratory, Los Alamos, NM 87544 USA*

(Dated: November 12, 2015)

Wendelstein 7-X aims to demonstrate the reactor capability of the stellarator concept, by creating plasmas with pulse lengths of up to 30 minutes at a heating power of up to 10 MW. The divertor plasma facing components will see convective steady state heat flux densities of up to $10\,MW/m^2$. These high heat flux target elements are actively cooled and are covered with CFC as plasma facing material. The CFC is bonded to the CuCrZr cooling structure. Over the life time of the experiment this interface may weaken and cracks can occur, greatly reducing the heat conduction between the CFC tile and the cooling structure. Therefore, there is not only the need to monitor the divertor to prevent damage by overheating, but also the need to detect these fatigue failures of the interface. A method is presented for an early detection of fatigue failures of the interface layer, solely by using the information delivered by the IR-cameras monitoring the divertor. This was developed and validated through experiments made with high heat flux target elements prior to installation in W7-X.

[a)]Electronic mail: Alexander.Rodatos@ipp.mpg.de

I. INTRODUCTION

Wendelstein 7-X (W7-X), an optimized modular stellarator, will be one of the very first experiments that will generate quasi-steady-state plasmas with fusion relevant parameters. The device will have discharge durations of up to 30 minutes and continuous injected power of up to 10 MW. W7-X is designed with low Z (low atomic number) plasma facing components (PFCs) to reduce the plasma radiation due to impurities. Consistent with the five-fold symmetry of the magnetic configuration, the experiment is divided into five nearly identical parts[9]. Each of these modules contains two divertor units and each unit is composed of different areas, capable of dissipating different heat flux densities (further called heat flux) depending on the expected loading. The largest is the so-called high heat flux (HHF) target area, designed for steady-state heat fluxes of up to $10\,MW/m^2$.

One of the major challenges for this experiment is a reliable and continuous operation to demonstrate the reactor capability of the stellarator concept. The plasma facing components (PFCs), especially the highly heat loaded *divertor*, responsible for particle and power exhaust, need to be monitored for operating the experiment safely. The HHF target area is built from 10 target modules, each of which in turn consists of 8 to 12 target elements. These target elements are of different types, which are 250 mm to 600 mm long and have a width of 50 mm to 61.5 mm. On the plasma-facing side they are covered with about 16000 tiles, 8 mm thick, made from carbon fibre reinforced carbon (CFC). In the case of W7-X CFC NB-31 is used[24]. The cooling structures of these elements are water-cooled CuCrZr heat sinks[5](See Figure 8). Due to different thermal expansion coefficients of Cu and CFC, a compliant layer is needed as an interface.

Experience with similar technology from Tore Supra showed that the performance of the divertor targets deteriorated in some cases[6,22]. Therefore a lot of effort was spent to improve the technology for use at W7-X. Analysis of the tiles with less performance showed cracks in the interface layer. We name the interfaces showing these cracks *delaminated*; they show strongly reduced heat conductivity between the CFC tile and the heat sink. At the tile edges these defects appear as macroscopic cracks in the interface layer and can be detected by visual inspection[4]. Under heat load, delaminated areas will show elevated surface temperatures and the thermomechanical stress induced by high heat loads (e.g. at

Figure 1: Pre series II divertor target elements.

$q_{surf} > 8$ MW/m^2), may cause a propagation of the delaminated interface area with every further heat cycle. For heat fluxes below $8\,MW/m^2$ no crack propagation was observed while for higher heat fluxes the crack propagation was strongly reduced in comparison to early designs of the interface layer[12].

W7-X is equipped with an in-vessel set of control coils allowing one to manipulate the strike line position and by that preventing excessive heat loads on delaminated tiles. A prerequisite to avoid further growth of the delaminated area by moving the strike line away is to identify those defects, before they reach sizes which could compromise safe operation. Therefore, in order to avoid such failures, a divertor surveillance system is under development at W7-X, whose central hardware components are 10 endoscope systems using infrared cameras operating in the wavelength range of $3\,\mu m$ to $5\,\mu m$. Each endoscope system is designed to observe the entire divertor with a spatial resolution of $6\,$mm to $10\,$mm on the divertor surface[7,19,20]. For a typical CFC tile size of 25 x 50 mm this is barely enough to resolve its surface temperature.

Experience from other fusion experiments shows that the observed infrared emission from a

PFC does not unambiguously allow a determination whether a very high infrared emission rate is caused by an unusually large incident heat load, a partially or fully delaminated tile, or a surface effect. Therefore it is mandatory to take the temporal evolution of the surface temperature into account when determining the state of the observed PFC (as discussed in[1,15,16,21,22]). It is also sketched in Figure 2. The three parts of the Figure shown represent the three basic cases that are of particular interest to us for the divertor in W7-X:

I: An intact, virgin tile with a good contact to the underlying cooling structures (left column in Figure 2).

II: A delaminated tile, a tile for which a smaller or larger part of the CFC has been disconnected from the cooling structure due to one or several cracks (middle column in Figure 2).

III: A tile with a surface layer. Such layers can appear on both intact and delaminated tiles. Depending on the plasma facing material (PFM) used the microstructures could also result in surface temperature much higher than the bulk temperature (right column in Figure 2)[15].

This work focuses on developing a robust and reliable criterion for safe-guarding and diagnosing the divertor in real-time using the infrared security system described above. First in Section II our approach is quantified by introducing a finite element model for heat transport inside intact and delaminated tiles. In Section III we analyze experimental data and develop the criterion to distinguish between intact and defective tiles. One of the major challenges using infrared surveillance of PFCs in magnetic fusion devices with carbon as plasma-facing material (PFM) comes from the formation of surface layers. In W7-X we expect mostly soft and hard amorphous carbon-hydrogen compounds (a-C:H) forming those layers. In Section IV we test if the developed criterion work in the presence of artificially introduced surface layers. Finally, the conclusions are presented in Section V.

II. FEM CALCULATIONS

The calculations using the finite element method (FEM) were performed with ANSYS using a model of the high heat flux targets[23] for W7-X. Since steady state heat loads up to
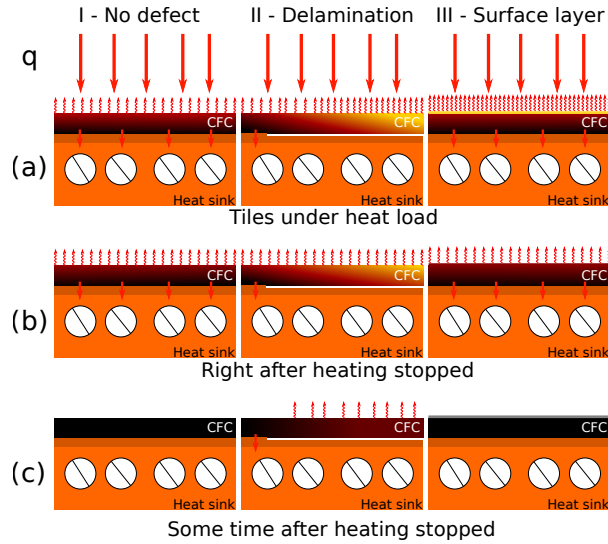
Figure 2: Sketched CFC-tile temperature (a) during the steady state phase, (b) right after the heat flux to the surface was stopped and (c) some time into the cooling of the target tiles. The straight red arrows represent the heat flux q. In case II the heat removal capacity is reduced because of the damaged interface. Heat removal is only possible over the part of the interface that is still intact causing much longer equilibration times depending on the size of the defect.
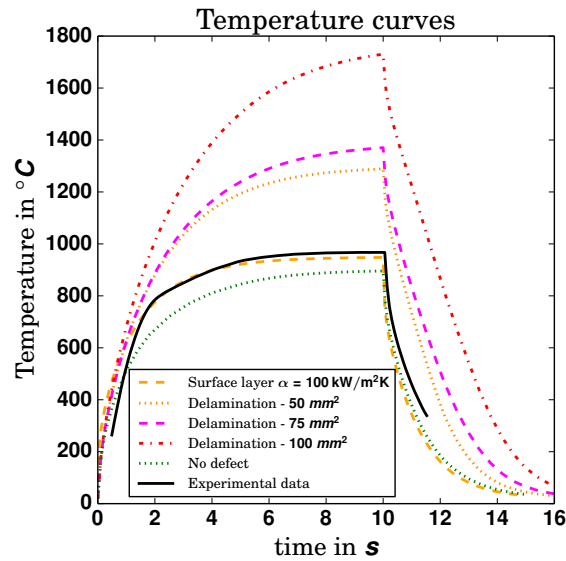

Figure 3: Surface temperature curves for tiles of different status. Data was gained by FEM calculations. Heating was switched off at $t_{off} = 10$ s. The different transient behaviour for target tiles with a surface layer, delamination or intact are visible. The experiment from which the experimental data (continuous line) are taken is described in section IV. The experimental temperature curves represent a case with no surface layer and no delamination.

$10\,MW/m^2$ are expected at W7-X, this value was used in the calculations. The temperature gradient is established within $10\,s$, therefore a pulse duration of $10\,s$ was chosen. The heat flux was distributed uniformly over the target surface. In order to simplify the calculations, only two mechanisms of cooling were considered: conductive transport from the tile surface towards the cooling channels and radiation losses from its surface. The model of the target element was adapted to include delamination defects and surface layers. In order to represent delaminated areas in the ANSYS code, the thermal connection between CFC material and the heat sink was removed. Delaminated areas of different size were simulated, in order to study the influence of defect size on the cooling behaviour.

In order to represent the surface layer in the model, a thin layer (thickness of $0.01\,mm$) with a specific heat capacity of $1000\,J/kgK$, a density of $1.9\,g/cm^3$ and a thermal conductivity of $1\,W/mK$ was added at top of the tile surface. This corresponds to a heat transmission coefficient α of $100\,kW/m^2K$ which is in the range of α-values found in other experiments[1,2]. The upper mesh size limit is $1\,mm$ for the CFC-Tile, $2\,mm$ for the heat sink and $0.05\,mm$ for the surface layer. Figure 3 presents modelled surface temperature for several cases of intact and delaminated tiles (see caption) as well as experimental data. The temperature for the delamination was taken at a fixed position $6\,mm$ inward from the lower edge and $2.5\,mm$ from the edge facing the neighbouring tile. In the case of no defects the surface temperatures was calculated at the center of the target tile.

To characterize the different transient surface temperature we used the following approach. A temperature decay time τ was used and is defined as:

$$\tau(t) = -\frac{T(t) - T_{coolant}}{\frac{dT(t)}{dt}} = -\frac{T(t_i) - T_{coolant}}{\frac{T(t_i) - T(t_{i+1})}{t_i - t_{i+1}}}. \tag{1}$$

with $T(t)$ as the measured surface temperature. τ allows us to get the characteristic time scale for the cooling process independent of the absolute temperature. A somewhat similar method has been published previously [22]. In that paper, however, the characteristic time τ was defined by the equation $T(\tau) - T_{\mathrm{coolant}} = 0.66(T_{\mathrm{max}} - T_{\mathrm{coolant}}$, whereas our definition is a continuous function of time. For a simple exponential temperature decay, the two definitions are about a factor of two different but otherwise very similar. However, for more complicated temporal evolution of the temperature, eg. if there are two disparate temporal time scales at play simultaneously, our τ captures both. As we will show in this
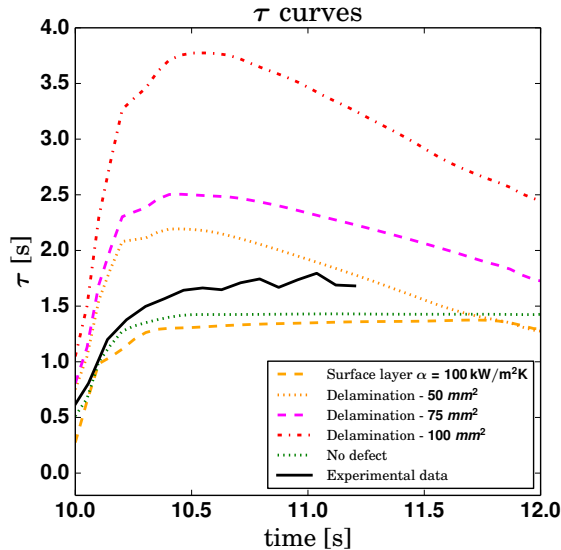
Figure 4: τ for the different cases. Beam off at $t_{off} = 10\,\text{s}$. The different states of the CFC-tile interface are clearly distinguishable by the different evolution of τ. While the surface layer has rather small influence on τ.

paper, it is possible to detect a delamination regardless of the presence of a surface layer. Figure 4 shows the evolution of τ for all the discussed cases. After the heating is stopped, $(t_{off} = 10\,\text{s})$ τ increases strongly. In the case of the intact tile and the tile with the surface layer, τ become constant afterwards, while in the case of delamination a maximum value is reached and after a short flat-top phase, τ begins to drop again. The height of the maximum increases with the size of the delaminated area. This is a result of the decreased overall heat transport from the tile to the heat sink for growing defect size. For comparing different cases $\tau(t = 10.5\,\text{s})$ from the flat-top phase is used, since any presence of a surface layer does not influence τ appreciably in this phase, and a clear difference between intact and delaminated tile can be identified. A difference of about 10 % between experimental data and FEM calculation in case of the steady state surface temperature is visible in Figure 3 and for the value $\tau(t = 10.5\,\text{s})$ the difference between experimental data and FEM calculations is about 25 % . The difference in the surface temperature can be explained by microscopic effects at the surface as described in the literature[15] while the difference in τ may be the result of the inhomogeneous thermal properties of the CFC which are not reproduced in the FEM calculations.

Table I: Values of $\tau(t = 10.5\,\text{s})$ for the different cases shown in figure 4

Case	$\tau(t = 10.5\,\text{s})[s]$
No defect	1.24
Experimental data	1.64
Delamination $50\,\text{mm}^2$	2.19
Delamination $75\,\text{mm}^2$	2.5
Delamination $100\,\text{mm}^2$	3.77
Surface layer	1.30

III. DISTRIBUTION OF DECAY TIME τ IN THE EXPERIMENTAL DATA

In a first step, archive data from HHF loading experiments at GLADIS (**G**arching **LA**rge **DI**vertor **S**ample Test Facility)[10] were used to verify the findings from the FEM calculations. In GLADIS, samples can be exposed to heat loads from $2\,MW/m^2$ to $55\,MW/m^2$ for pulse lengths of up to $30\,\text{s}$. The main mission of the device is to qualify and test plasma-facing components under realistic load conditions, and has been used extensively during the development and qualification of the W7-X HHF divertor elements. Two hydrogen neutral beams are available with a Gaussian heat flux profile of $100\,\text{mm}$ mean width diameter at the target position. The target is observed by cameras operating in the visible and infrared range. A detailed description of the GLADIS facility and further available diagnostic can be found in[11]. The infrared archive data have a frame rate of $10\,\text{Hz}$ and a spatial resolution of $1\,\text{mm/px}$. Observations were made in the wavelength range of $8\,\mu m$ to $12\,\mu m$.

For the final qualification of the W7-X target elements, prototype elements were exposed to a heat flux of $10.5\,MW/m^2$ for $10\,\text{s}$ with variation of the beam intensity $< 5\,\%$ between two heat cycles[13]. In case of an intact interface the surface temperature reached $99\,\%$ of $T_{max} - T_{coolant}$ after $7\,\text{s}$, well within the exposure time of typical $10\,\text{s}$. The inlet temperature of the cooling water was $\sim 20\,°C$ with a velocity of $8\,\text{m/s}$ and a static pressure of $1\,\text{MPa}$. Target tiles were loaded between 100 to 10.000 cycles. To determine whether the interface of the target tile met the specifications the surface temperature difference between the tile edges and the center was evaluated over a large number of heat cycles. If the temperature difference has grown more than $75\,\text{K}$ after 100 cycles the tile was declared defect. The exact description of these experiments can be found in reference[13] . IR camera data are available for a number of these tests. We used these records to study the evolution of the surface
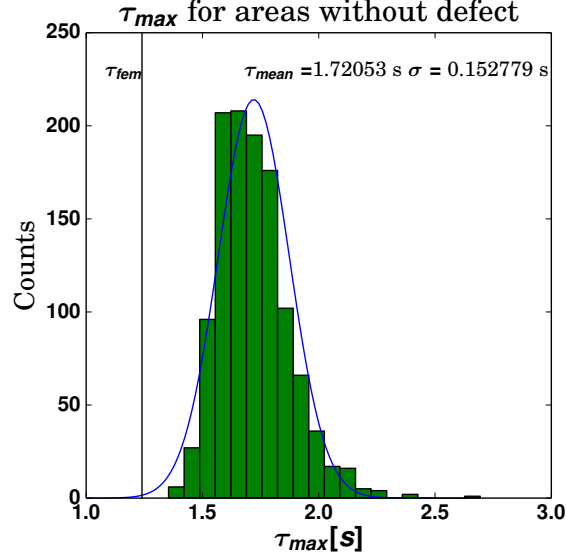
Figure 5: Distribution of τ_{max} for ROIs without known defects. Results from the qualification tests were used to sort out tiles with defects. $\tau_{mean} = 1.72\,\text{s}$ with $\sigma = 0.15\,\text{s}$. For comparison also $\tau_{fem} = 1.24\,\text{s}$, from FEM case with no defect, is shown.

temperature during the transient phases of cooling and heating, so as to gain statistics on intact tiles under high loads. On each target element, three regions of interest were defined, each of them covering about 1/3 of a tile: the first region covered the upper edge, the second one covers the target's center, and the last one the lower edge (see figure 8). Each region has a size of 15 mm times 20 mm and includes approximately 300 pixels. For each pixel τ was calculated after smoothing the temperature curves. A Blackman window[14] with a width of 5 frames was used. To further reduce the noise τ was averaged over three time frames:

$$\tau = \frac{\tau_{i-1} + \tau_i(t \approx 10.5\,\text{s}) + \tau_{i+1}}{3} \tag{2}$$

Here i denotes the frame number. For each region of interest the highest value of τ was taken. The resulting distribution of τ_{max} for all regions of interest with no known error is shown in figure 5. The mean value of this distribution is $\tau_{mean} = 1.72\,\text{s}$ with $\sigma = 0.15\,\text{s}$. For three known defects τ also was determined and compared to τ_{mean}. The three defects A,B and C were detected on different prototype target elements. Defect A and C were band defects on the edge of the target tiles and defect B was a corner defect. While for error A and B the CFC tile with the cooper interlayer was connected via electron beam welding (EBW) to the heat sink, hot isostatic pressing (HIP) was used for the interface in case of
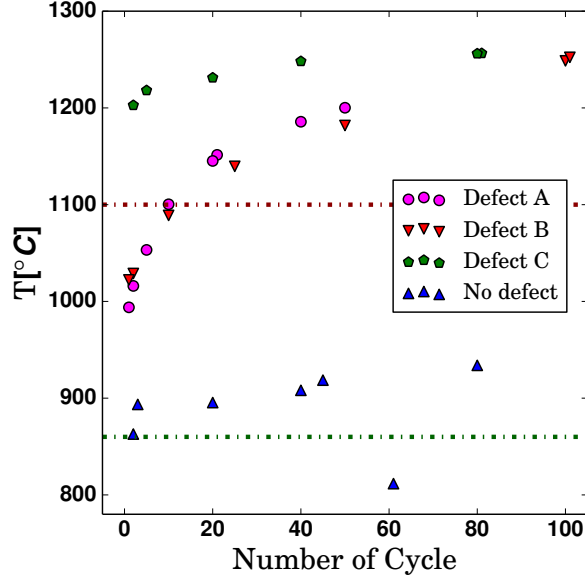
9

Figure 6: Steady state surface temperature for tiles exposed to a heat flux of $10.5\,MW/m^2$ (5% fluctuation). The surface temperature for non-defect tiles is in the range between $860\,^\circ C$ and $1100\,^\circ C$. An increase of the surface temperature is for all cases visible and two kinds of defects are visible: Fast-growing (Defect A and B), and slowly-growing (Defect C).

error C[3]. All of these defects are smaller than $20\,\%$ after 100 heat cycles. These errors developed differently over the number of heat cycles and are discussed bellow.

In figure 6 the local surface temperature of the three defects and for one tile without a defect are shown. When an intact target tile is loaded with $10.5\,MW/m^2$ the surface temperature typically varies between $860\,^\circ C$ and $1100\,^\circ C$[10] due to the scatter of CFC material properties[15,18]. From the evolution of the surface temperature two different behaviours in case of defects can be deduced. Defects A and B show during the first heat cycle a surface temperature similar to an intact tile. However, during the following heat cycles the surface temperature increases rapidly until approximately 30th heat cycles ($\Delta T|_{1to30} = 130\,\mathrm{K}$) and increases slowly after wards ($\Delta T|_{30to100} = 90\,\mathrm{K}$). Defect C shows a surface temperature beyond $1100\,^\circ C$ from the beginning and a slow but constant temperature increase for the following heat cycles ($\Delta T|_{1to80} = 30\,\mathrm{K}$). For the same cases the decay-times τ are shown in figure 7. The distribution of decay-times for tiles without defects is shown in the background of the figure. Case A,B and C show a growing decay-time with the number of cycles. Also the decay-time trend shows a good agreement with the trend for the surface temperatures. We can distinguish between two types of defects: For defect C the interface was damaged
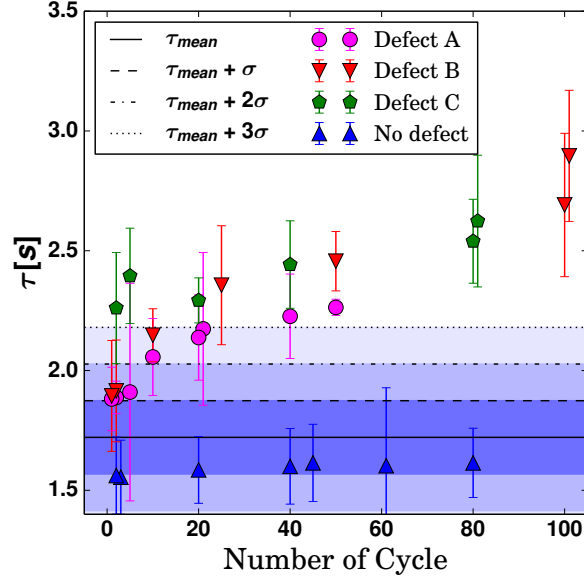
Figure 7: Decay time τ_{delam} for known defects. The growth of the delaminated areas is represented in the increase of τ_{delam} over the number of heat cycles. In the background the distribution of τ from 5 is shown. The coloured areas represent the one σ (dark blue) and two σ (lighter blue) and three σ (faint blue) range.

from the beginning, which could be a production error. The interface of this defect was created by HIP and is growing slowly. Defects A and B are examples of the second type, where the interface was created by EBW: these show an accelerating growth of the defect for the first heat cycles and a steady but sustained growth in subsequent heat cycles. These rapidly growing defects are critical for the lifetime of the divertor. The number of heat cycles onto tiles with such defects must be reduced as much as possible in order to allow for a long life. It should be mentioned here, that we measured the presented defects in an early prototype phase only. These kind of errors did not occur for the manufactured HHF targets, due to the higher quality of manufacturing of the final interface design[13].

IV. DETECTION OF TILE DEFECTS IN THE PRESENCE OF SURFACE LAYERS

To investigate if defective tiles are still detectable by the τ-criterion ($\tau_{delam} > \tau_{mean} + 3\sigma$) in the presence of surface layers, one prototype target element with artificial amorphous hydrocarbon (a-C:H) layers was tested at GLADIS. The most common mechanism of surface layer formation is the re-deposition of eroded material from the PFCs. In a hydrogen-isotope

Figure 8: Example of a prototype of the W7-X divertor target element. It consists of 10 CFC tiles (with a thickness of 8 mm, a length of $\approx 25\,$mm and a width of $\approx 55\,$mm) bonded to a water-cooled CuCrZr heat sink. The numbers indicated on the tile surfaces denote thickness of the a-C:H surface layers used to emulate real surface layers building up during the W7-X operation. On tile 9 the regions of interest used for the data evaluation are shown.

plasma device with carbon as the main PFM, surface layers consist mostly of a-C:H. Traces of metallic components can also be found in such surface layers[17], if metal (typically steel) components are also exposed directly or indirectly to the plasma.

The target element used for these experiments had already been exposed to heat flux prior to our experiments at least a hundred times, straining the interface between CFC tile and heat sink. Several tiles have known and well-characterized defects which were documented during the qualification tests (see section III). To determine the influence of surface layers on detecting defective interfaces, we exposed the tiles before coating them, to a heat flux of $8.5\,$MW/m^2. These experiments were performed directly after the commissioning of GLADIS after a prolonged shut down, therefore the calibration of the ion sources changed resulting in the lower power density. The average τ was measured for the center, the top and lower edge of the tiles. Figure 9 a shows the decay times for the reference shots. Afterwards four tiles were coated with a-C:H layers of different thickness ($1\,\mu m$, $2\,\mu m$, $4\,\mu m$, $8\,\mu m$) at IPP Garching. They were exposed to a heat flux of $10.5\,MW/m^2$ for $10\,$s. For some tiles, the measured surface temperature rose to $1600\,°C$. The results for τ can be seen in figure 9 b.

In Figure 10 an overview of the tile state determined by our reference experiment and a comparison with the results from the GLADIS qualification tests is shown (see III). During the qualification tests tile 3,4 and 7 were determined to likely be defect and tile 5 and 6 were classified defective. In our experiments tile 3 to 5 and 7 to 8 were classified as defective,

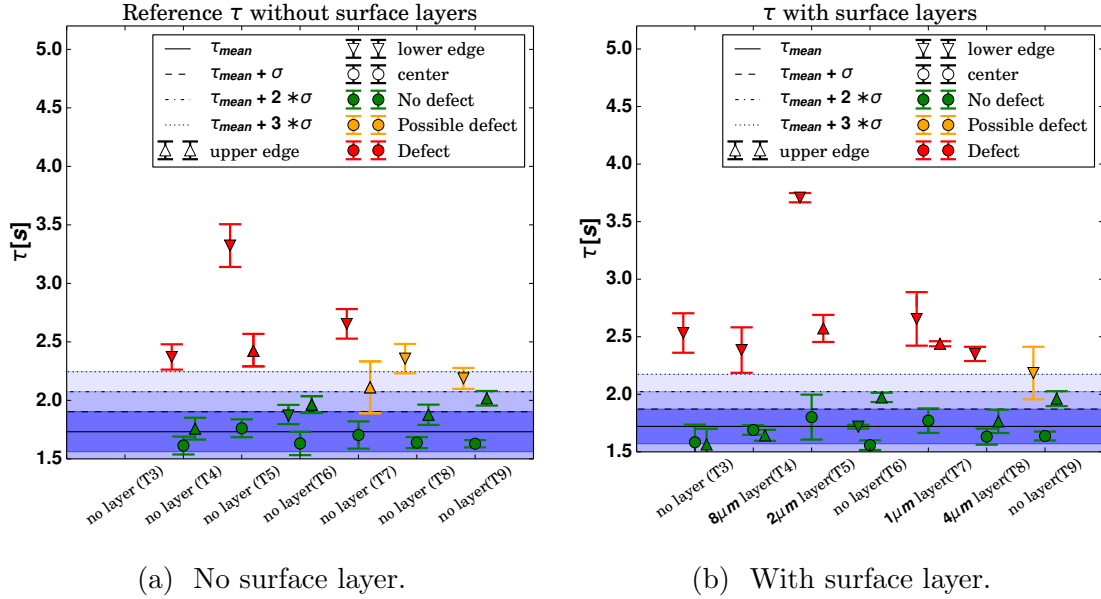(a) No surface layer.   (b) With surface layer.

Figure 9: Decay times for known defects without (a) and with (b) surface layers. For the different target tiles (x-axis) the decay times for the center, and both edges are shown. For clarity the three data points for each ROI are shifted horizontally. Notice that the presence of the surface layer does not hinder the detection of the defects. For the experiment without a surface layer no data for tile 3 is available.

while tile 6 showed only a slight increase in τ at the upper edge. Visual inspection of the interfaces[4] of the tiles revealed, that the interface of tile 6 shows only a small crack at the lower interface. This crack also is not continuous over the area which could explain the small increase of τ. Nevertheless the surface temperature of tile 6 is greater than $1100\,°C$, which still is within the scatter of the CFC properties but higher than the allowed surface temperature. While the cause of the increased surface temperature needs to be further investigated it represents no threat to the safe operation of the machine.

The results do not change significantly when surface layers are added. The measured surface temperature rose for tile 8 ($4\,\mu m$ - layer) and some hot spots on tiles 5 and 4 up to $1600\,°C$. These hot spots are areas where the a-C:H layer is much thicker than anticipated. Nevertheless the results for τ show no significant deviation from the experiments without surface layers (see figure 9).

		Target tiles						
		3	4	5	6	7	8	9
Results from qualification tests at GLADIS		yellow	yellow	red	red	yellow	green	green
Results from τ- criteria	upper Edge	green	green	red	green	red	green	green
	lower Edge	red	red	red	green	red	red	yellow
visual inspection	upper Edge	green	green	red	green	red	green	green
	lower Edge	red	red	red	yellow	red	yellow	yellow

Figure 10: Overview of tile states found during the qualification tests, our experiments and visual inspection. Green indicates intact bonds, yellow are questionable, and red indicates defects. The visual inspection is in good agreement with our findings while there is a discrepancy between our experiments and the results from the qualification experiments. They are discussed in the text.

V. CONCLUSION AND OUTLOOK

It has been shown that it is possible to detect delamination defects for W7-X target elements exposed to power fluxes compatible with stead-state conditions of W7-X. The method developed in this work allows to ignore surface layers when detecting delaminations. The τ-criterion based solely on infrared camera measurements imposes relatively low computational effort for the image analysis. Thus, the structural health of the divertor tiles can be determined in situ, and essentially in real-time, by comparing the temperature decay time τ of a pixel to the known distribution of τ for intact tiles. The criterion require a modulation in the local heat fluxes onto the components, in order to diagnose the health condition of divertor tiles during plasma operation. Therefore, plasma discharge scenarios must be developed that modulate the local divertor heat loads in a controlled way, without negatively affecting the plasma performance. The so-called control coils[8] are expected to be able to provide this modulation.

The criterion is already implemented in a fully automated computer algorithm that gives robust results. Future work is needed to implement the algorithm in a real-time system that has the needed response time. It is important to note, that the used IR-data have a significantly higher spatial resolution ($< 1\,\mathrm{mm/px}$) compared to what will be available for

14

W7-X (6-10 mm). The lower available resolution on W7-X will reduce the sensitivity of the method and the minimum size of a detectable delamination. Therefore, the effectiveness of the algorithm must be tested for a situation with a realistic spatial resolution and potentially developed further if the performance is significantly degraded as a result.

ACKNOWLEDGMENTS

REFERENCES

[1] P. Andrew, J.P. Coad, Y. Corre, T. Eich, A. Herrmann, G.F. Matthews, J.I. Paley, L. Pickworth, R.A. Pitts, and M.F. Stamp. Outer divertor target deposited layers during reversed magnetic field operation in {JET}. *Journal of Nuclear Materials*, 337–339(0):99 – 103, 2005. PSI-16.

[2] P. Andrew, J.P. Coad, T. Eich, E. Gauthier, A. Herrmann, G.F. Matthews, V. Riccardo, and M. Stamp. Thermal effects of surface layers on divertor target plates. *Journal of Nuclear Materials*, 313–316(0):135 – 139, 2003. Plasma-Surface Interactions in Controlled Fusion Devices 15.

[3] J Boscary, B Böswirth, H Greuner, P Grigull, M Missirlian, A Plankensteiner, B Schedler, T Friedrich, J Schlosser, B Streibl, and H Traxler. Fabrication and testing of w7-x pre-series target elements. *Physica Scripta*, 2007(T128):195, 2007.

[4] J. Boscary, A. Peacock, M. Smirnow, and H. Tittes. Summary of research and development activities for the production of the divertor target elements of wendelstein 7-x. *Plasma Science, IEEE Transactions on*, 42(3):533–538, March 2014.

[5] J. Boscary, R. Stadler, A. Peacock, F. Hurd, A. Vorköper, B. Mendelevitch, A. Cardella, H. Pirsch, H. Tittes, J. Tretter, C. Li, H. Greuner, and M. Smirnow. Design and technological solutions for the plasma facing components of wendelstein 7-x. *Fusion Engineering and*

Design, 86(6–8):572 – 575, 2011. Proceedings of the 26th Symposium of Fusion Technology (SOFT-26).

[6] Laizhong Cai, Eric Gauthier, Yann Corre, Thierry Loarer, Marc Missirlian, Vincent Martin, and Victor Moncada. Evolution of the bonding defect reported on the tiles of the toroidal pumped limiter of the tore supra tokamak with infrared analysis. *Physica Scripta*, 85(1):015501, 2012.

[7] J. Cantarini, D. Hildebrandt, R. König, F. Klinkhamer, K. Moddemeijer, W. Vliegenthart, and R. Wolf. Optical design study of an infrared visible viewing system for wendelstein 7-x divertor observation and controla). *Review of Scientific Instruments*, 79(10):–, 2008.

[8] F. Füllenbach, Th. Rummel, S. Pingel, H. Laqua, I. Müller, and E. Jauregi. Final test of the w7-x control coils power supply and its integration into the overall control environment. *Fusion Engineering and Design*, 82(5–14):1391 – 1395, 2007. Proceedings of the 24th Symposium on Fusion Technology SOFT-24.

[9] Maurizio Gasparotto, Christophe Baylard, Hans-Stephan Bosch, Dirk Hartmann, Thomas Klinger, Reinhard Vilbrandt, and Lutz Wegener. Wendelstein 7-x—status of the project and commissioning planning. *Fusion Engineering and Design*, 89(9–10):2121 – 2127, 2014. Proceedings of the 11th International Symposium on Fusion Nuclear Technology-11 (ISFNT-11) Barcelona, Spain, 15-20 September, 2013.

[10] H. Greuner, B. Boeswirth, J. Boscary, and P. McNeely. High heat flux facility gladis:: Operational characteristics and results of w7-x pre-series target tests. *Journal of Nuclear Materials*, 367–370, Part B(0):1444 – 1448, 2007.

[11] H. Greuner, H. Bolt, B. Böswirth, T. Franke, P. McNeely, S. Obermayer, N. Rust, and R. Süß. Design, performance and construction of a 2mw ion beam test facility for plasma facing components. *Fusion Engineering and Design*, 75–79(0):345 – 350, 2005. Proceedings of the 23rd Symposium of Fusion Technology {SOFT} 23.

[12] H. Greuner, B. Böswirth, J. Boscary, P. Chaudhuri, J. Schlosser, T. Friedrich, A. Plankensteiner, and R. Tivey. Cyclic heat load testing of improved cfc/cu bonding for the w 7-x divertor targets. *Journal of Nuclear Materials*, 386–388(0):772 – 775, 2009.

[13] H. Greuner, U.v. Toussaint, B. Böswirth, J. Boscary, H. Maier, A. Peacock, and H. Traxler. Performance and statistical quality assessment of {CFC} tile bonding on the pre-series elements of the wendelstein 7-x divertor. *Fusion Engineering and Design*, 86(9–11):1685 – 1688, 2011. Proceedings of the 26th Symposium of Fusion Technology (SOFT-26).

[14] F.J. Harris. On the use of windows for harmonic analysis with the discrete fourier transform. *Proceedings of the IEEE*, 66(1):51–83, Jan 1978.

[15] A Herrmann. Surface temperature measurement and heat load estimation for carbon targets with plasma contact and machine protection. *Physica Scripta*, 2007(T128):234, 2007.

[16] D. Hildebrandt and A. Duebner. Thermal response of structured and contaminated carbon surfaces to heat pulses. *Journal of Nuclear Materials*, 363–365(0):1221 – 1225, 2007. Plasma-Surface Interactions-17.

[17] D. Hildebrandt, A. Dübner, H. Greuner, and A. Wiltner. Thermal response to heat fluxes of the w7-as divertor surface submitted to surface modification under high temperature treatment. *Journal of Nuclear Materials*, 390–391(0):1118 – 1122, 2009. Proceedings of the 18th International Conference on Plasma-Surface Interactions in Controlled Fusion Device Proceedings of the 18th International Conference on Plasma-Surface Interactions in Controlled Fusion Device.

[18] D. Hildebrandt, D. Naujoks, and D. Sünder. Surface temperature measurements of carbon materials in fusion devices. *Journal of Nuclear Materials*, 337–339(0):1064 – 1068, 2005. PSI-16.

[19] M. W. Jakubowski, C. Biedermn, R. König, A. Lorenz, T. Sunn Pedersen, A. Rodatos, and Wendelstein 7-X team. Development of infrared and visible endoscope as the safety diagnostic for steady- state operation of wendelstein 7-x. In *Conference QIRT 2014 (Bordeaux, France), 7-11 July 2014*, volume QIRT-2014-100, Conference QIRT 2014 (Bordeaux, France), 7-11 July 2014, July 2014.

[20] R. König, D. Hildebrandt, T. Hübner, F. Klinkhamer, K. Moddemeijer, and W. Vliegenthart. Optical design study for divertor observation at the stellarator w7-x. *Review of Scientific Instruments*, 77(10):–, 2006.

[21] C. Martin, R. Ruffe, C. Pardanaud, M. Cabié, C. Dominici, T. Dittmar, P. Languille, B. Pégourié, E. Tsitrone, and P. Roubin. Structure of the carbon layers deposited on the toroidal pump limiter of tore supra. *Journal of Nuclear Materials*, 415(1, Supplement):S258 – S261, 2011. Proceedings of the 19th International Conference on Plasma-Surface Interactions in Controlled Fusion.

[22] R Mitteau, J C Vallet, R Reichle, C Brosset, P Chappius, J J Cordier, E Delchambre, F Escourbiac, A Grosman, D Guilhem, M Lipa, T Loarer, J Schlosser, and E Tsitrone.

Evolution of carbon tiles during repetitive long pulse operation in tore supra. *Physica Scripta*, 2004(T111):157, 2004.

[23] X.B. Peng, V. Bykov, M. Köppen, M.Y. Ye, J. Fellinger, A. Peacock, M. Smirnow, J. Boscary, A. Tereshchenko, and F. Schauer. Thermo-mechanical analysis of wendelstein 7-x plasma facing components. *Fusion Engineering and Design*, 88(9–10):1727 – 1730, 2013. Proceedings of the 27th Symposium On Fusion Technology (SOFT-27); Liège, Belgium, September 24-28, 2012.

[24] G Pintsuk, J Compan, J Linke, P Majerus, A Peacock, D Pitzer, and M Rödig. Mechanical and thermo-physical characterization of the carbon fibre composite nb31. *Physica Scripta*, 2007(T128):66, 2007.